J|A|C|S COMMUNICATIONS

Published on Web 10/20/2010

Assessing the Purity of Metal−Organic Frameworks Using Photoluminescence: MOF-5, ZnO Quantum Dots, and Framework Decomposition

Patrick L. Feng, John J. Perry IV, Stefan Nikodemski, Benjamin W. Jacobs, Scott T. Meek, and Mark D. Allendorf*

Sandia National Laboratories, Livermore, California 94551-0969

Received July 23, 2010; E-mail: mdallen@sandia.gov

Abstract: Photoluminescence (PL) spectroscopy was used to characterize nanoscale ZnO impurities, amine-donor charge-transfer exciplexes, and framework decomposition in samples of MOF-5 prepared by various methods. The combined results cast doubt on previous reports describing MOF-5 as a semiconductor and demonstrate that PL as a tool for characterizing MOF purity possesses advantages such as simplicity, speed, and sensitivity over currently employed powder XRD MOF characterization methods.

Metal−Organic Frameworks (MOFs) are the subject of intense recent interest due to their diverse properties and highly tunable construction. Numerous uses have been investigated, including, but not limited to, gas storage/separations, sensing, catalytic, optical, and electronic applications. Phase-pure materials are essential for both understanding MOF behavior and for designing MOFs for specific applications. Unfortunately, high purity can be difficult to obtain, due to the large void spaces in MOFs, one-pot solvent-based synthetic procedures, and partial structural collapse that can occur upon removal of guest molecules. Powder XRD is typically used to characterize the purity of MOFs, although this technique is of limited utility to detect amorphous or weakly crystalline impurities. The present work demonstrates that photoluminescence spectroscopy, a commonly available laboratory diagnostic, is a very sensitive probe of trapped solvent and framework decomposition products and provides a more reliable assessment of MOF purity. We chose MOF-5 (also known as IRMOF-1) as a case study because its properties, particularly surface area, are known to be highly sensitive to the preparation method.[1−6] Moreover, it continues to be heavily studied and therefore merits a thorough investigation of its luminescent properties, which to date has not been performed.

Providing an additional motivation for this work are the multiple theoretical and experimental reports that some MOFs behave as nanoscale semiconductors and photocatalysts as a result of their hybrid structure comprising organic linkers and metal-cluster nodes.[7−14] In particular, the archetypical MOF-5 has been labeled a ZnO-like semiconductor,[7−12] which conflicts with DFT calculations predicting it is an insulator and spectroscopic analysis indicating that luminescence in zinc carboxylate MOFs is ligand-centered.[15,16] Nonetheless, it has been suggested that the luminescence and semiconductor behavior of MOF-5 arises from a $O^{2-}Zn^{2+}\rightarrow O^{-}Zn^{+}$ charge-transfer transition within each tetrahedral Zn_4O_{13} metal cluster, which has been described as ZnO-like quantum dots.[7−11] Intense photoluminescence excitation/emission was observed at 350 nm/525 nm, which was ascribed to energy harvesting and ligand-to-metal charge transfer (LMCT) from the 1,4-benzenedicarboxylate (BDC^{2-}) linkers to the Zn_4O_{13} cluster.[7]

All reports describing MOF-5 semiconductivity[7−11] employ the widely used direct-mixing synthetic procedure reported by Huang et al.[4] (MOCP-L), which was subsequently shown to yield a significantly reduced surface area and adsorption capacity in comparison to well-characterized, high-surface-area single-crystal samples produced by other methods.[1−3,5,6] In detailed work by Hafizovic and Calleja, these discrepancies are explained in the context of framework interpenetration and the presence of trapped organic and zinc species.[1,3] The trapped inorganic species were tentatively assigned as $[Zn(OH)_2(H_2O)_2]$ on the basis of disordered residual electron density within the MOF pores in single-crystal X-ray diffraction experiments.[1] In this contribution we report the photoluminescence (PL) properties of MOF-5 prepared by various methods, emphasizing the use of fluorescence as a sensitive tool for the detection of multiple impurities that arise from commonly employed MOF synthetic methods. These results also cast considerable doubt on previous reports of MOF-5 as a semiconductor, as all previous observations may be explained by the presence of ZnO impurities serving as the photocatalytic and semiconducting species.

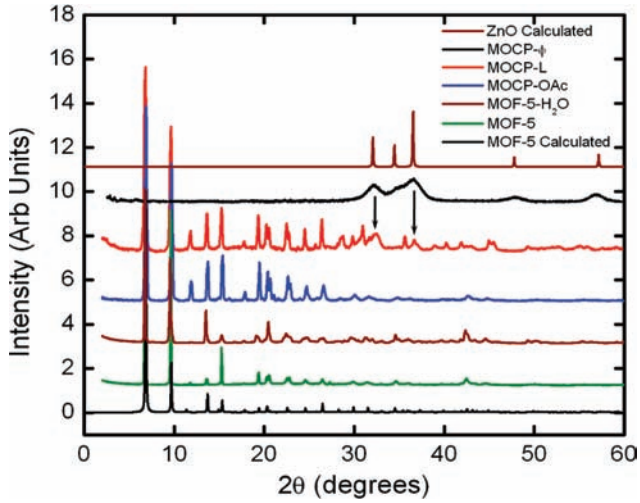

Figure 1. Powder X-ray diffraction data. Intensities for the MOF-5 samples are normalized to the diffraction peak at 6.74°. The patterns for ZnO (Wurtzite) and MOF-5 were calculated from single crystal structural data. Black arrows indicate ZnO diffraction peaks in MOCP-L.

MOF-5 was synthesized using four different methods, comprising direct-mixing precipitation methods reported by Huang et al.[4] (MOCP-L) and Tranchemontagne et al.[6] (MOCP-OAc), as well as solvothermal crystallization syntheses reported by Kaye et al.[5] (MOF-5, MOF-5-H_2O) and Li et al.[20] (MOF-5_{HT}) (Figure 1). Control reactions for each of the above syntheses were performed in the absence of H_2BDC, as $Zn(OAc)_2\cdot 2H_2O$ and $Zn(NO_3)_2\cdot 6H_2O$ are reported to yield monodisperse 2−4 nm ZnO nanoparticles upon dissolution and gentle heating to 50 °C in polar basic aprotic solvents such as DMF and DMSO.[22,23] Indeed, direct mixing of triethylamine (TEA) and $Zn(NO_3)_2\cdot 6H_2O$ in an 8:1 ratio in DMF

 © 2010 American Chemical Society

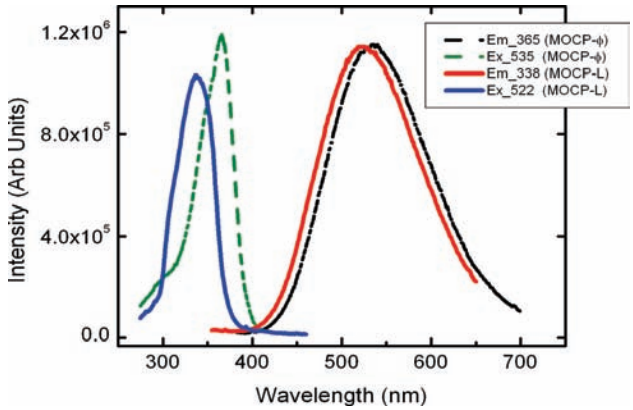

Figure 2. Comparison of the excitation and emission spectra for MOCP-Ø (dashed) and MOCP-L (solid).

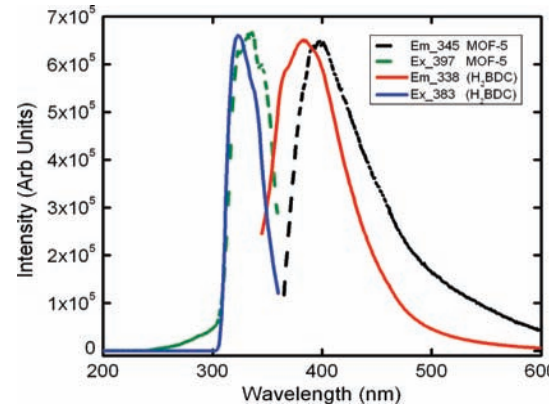

Figure 3. Comparison of the excitation and emission spectra for a dilute DMSO solution of H_2BDC (solid) and single crystals of MOF-5 (dashed).

results in the precipitation of a white colloidal suspension of ZnO, hereafter referred to as MOCP-Ø. These conditions are identical to those reported for MOCP-L, aside from the exclusion of H_2BDC. MOCP-Ø was determined to consist of nanoscale ZnO via powder XRD (*vide infra*). This material exhibits an intense luminescence at 535 nm upon excitation at 365 nm, which was previously assigned to the capture by trapped holes of photoexcited electrons from the conduction band that are associated with the singly ionized oxygen vacancies of surface states of ZnO (Figure 2).[21,23−25] This defect-related emission is related to the surface-to-volume ratio of ZnO, which increases with decreasing particle size.[23] Strong luminescence enhancement of up to 50× has been previously observed for nanoscale versus bulk ZnO, which accounts for the bright yellow fluorescence of MOCP-Ø and MOCP-L.[25] In contrast, the initial report of MOF-5 as a semiconductor cited the observed PL enhancement as evidence for an efficient energy transfer from the terephthalate linkers to the tetrahedral Zn_4O_{13} 'quantum dots'.[7]

Corresponding PL data were collected for MOCP-L, resulting in spectra that reproduce the results reported by Bordiga[1] and Tachikawa.[9] These spectra, also shown in Figure 2, are similar to those of MOCP-Ø, displaying strong visible emission at 522 nm upon UV excitation at 338 nm. However, the MOCP-L excitation and emission maxima are blue-shifted by 27 and 13 nm relative to MOCP-Ø, respectively. These observations are explained by taking into account the effects of particle size, which can be synthetically modified in both MOCP-Ø and MOCP-L by changing the quantity of solvent, rate of reagent addition, and stirring/storage time. The particle size distribution of these ZnO particles may be estimated from the excitation (Figure 2) and absorption (Figure S1) spectra by considering the effects of quantum confinement. It is known that these effects become operative when the size of a semiconductor particle becomes comparable to the exciton diameter, leading to size-dependent shifts in the absorbance and excitation spectra.[26] The average particle size may thus be estimated from the wavelength at the peak absorption in the PL excitation spectrum using the effective mass model (eq S1) for a monodispersed ZnO nanocolloid.

The respective excitation maxima for MOCP-L and MOCP-Ø occur at 338 and 365 nm, which are notably blue-shifted relative to bulk ZnO (390 nm). Figure S2 describes the ZnO particle diameter as a function of the peak excitation wavelength, indicating that the average ZnO particle size for samples of MOCP-L and MOCP-Ø is 5.0 and 3.6 nm, respectively. TEM analysis confirms these particles as 2−5 nm nanocrystals (Figures S5−S9), which is consistent with DMF-synthesized ZnO colloids, as well as ZnO nanoparticles synthesized inside MOF-5 crystals via gas-phase infiltration and subsequent oxidation of diethylzinc.[21,27] Independently, we find an average ZnO particle size in MOCP-Ø of 6 nm by applying the Scherrer equation to the powder XRD data in Figure 1. These size measurements indicate that the majority of ZnO particles are larger than the MOF pores and that the ZnO impurities exist primarily as extrinsic contaminants or particles extending across multiple framework cavities.

To eliminate possible charge-transfer and luminescence quenching effects of added TEA in the above synthesis, high- quality single crystals of MOF-5 were solvothermally synthesized at 80 °C from $Zn(NO_3)_2 \cdot 6H_2O$ and H_2BDC in DMF, yielding colorless and translucent cube-shaped crystals of MOF-5.[5] The resulting PL spectra are shown in Figure 3, revealing an excitation maximum at 345 nm and a single emission at 397 nm. The appearance of vibronic structure and symmetric nature of the excitation and emission spectra indicates that the luminescence originates from a single excited state. These observations contrast sharply with the spectra of MOCP-L, which are correlated with the purity of the MOF-5 samples with respect to ZnO contaminants and are much more intense than those of MOF-5. The MOF-5 PL data in Figure 3 are overlaid with the corresponding spectra for a dilute solution of H_2BDC in DMSO. The similarities between these spectra indicate linker-centered emission for MOF-5 that is free of intermolecular and charge-transfer interactions (LMCT). The very broad shoulder above ~430 nm in the emission spectrum for MOF-5 corresponds to a small amount of highly emissive framework decomposition impurity, as will be discussed below. Similar PL spectra were obtained for the high surface area MOF-5 product (MOCP-OAc)[6] synthesized via direct mixing of DMF solutions of H_2BDC and $Zn(OAc)_2 \cdot 2H_2O$, as well as for a 2:2:1 TEA:$Zn(NO_3)_2 \cdot 6H_2O$:H_2BDC variation of the original (8:2:1 reagent ratio) method reported by Huang.[4]

The above observations are not surprising considering the open framework structure and closed-shell Zn^{II} ions possess no metal-centered electronic states near the conduction band.[15] These results are also consistent with the linker-centered emission spectra obtained for a MOF composed of stilbenedicarboxylate linkers and Zn_4O subunits of the type found in IRMOFs.[16]

Since DEF is known to hydrolyze to produce formic acid and the electron donor diethylamine (DEA), single crystals of MOF-5 were synthesized from DEF at a higher temperature (110 °C) than that used by Kaye et al., analogous to the procedure reported by Li et al.[5,20,28] Millimeter-sized translucent orange cubes of MOF-5_{HT} were collected after heating for an extended period of 48 h and were washed exhaustively with DMF to remove surface impurities and residual DEF mother liquor. The orange color of MOF-5_{HT} cannot be removed via solvent exchange and is frequently observed in solvothermal MOF

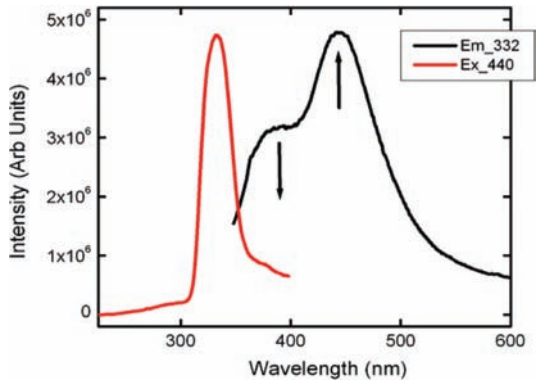

Figure 4. PL excitation and emission spectra for single crystals of MOF-5-H_2O synthesized solvothermally from a 50:1 mixture of DMF/H_2O at 100 °C according to the procedure by Kaye et al.[15] Black arrows indicate the spectral changes observed upon increasing exposure to moisture.

syntheses employing DEF at elevated temperatures.[3,5] The luminescence spectra of MOF-5_{HT} are presented in Figure S3, revealing a single intense emission at 493 nm upon excitation at 414 nm. These features are reminiscent of the formation of a charge-transfer exciplex between DEA and the terephthalate linkers, owing to the broad, featureless emission and excitation maximum in the visible region of the spectrum. Similar results are obtained by soaking pristine colorless crystals of MOF-5 in amine electron donors such as diethylaniline, leading to orange-colored crystals that absorb in the visible and emit at 550 nm (Figure S4).

In addition to detecting impurities, we find that framework decomposition of MOF-5 can be monitored using PL spectroscopy. An intense blue-green emission at 440 nm appears after exposure to atmospheric moisture (Figure 4). The decomposition of MOF-5 upon exposure to water (MOF-5-H_2O) is found to produce a nonporous phase that has been previously characterized via gas sorption measurements and powder XRD.[5,29] The sensitivity advantage of PL spectroscopy is apparent under these conditions, as appreciable luminescence from decomposed MOF-5 is observed even for samples that appear to be phase pure via powder XRD (Figures 1, 4). Indeed, the difficulty in obtaining pure material that exhibits only the violet luminescence associated with the BDC^{2-} linkers further attests to the appreciable moisture sensitivity of MOF-5. These results may also explain the wide variations in surface area/porosity reported for samples of MOF-5 having very similar powder XRD patterns. Work is in progress in our laboratory to quantify this effect and will be reported in a future publication.

The above PL results indicate that the MOCP-L material that is often assumed to be pure MOF-5 is contaminated with highly emissive ZnO nanoparticles, which is of particular concern for determining whether or not MOF-5 is a semiconductor. The presence of ZnO impurities may also account for multiple anomalous results such as the previously reported MOCP-L mediated photoreduction of methyl viologen[8,10] and photo-oxidation of phenols,[11] both in water, a solvent in which MOF-5 is known to rapidly decompose.[5,19,29] Similarly, the photovoltaic and electroluminescent properties previously reported are likely the result of ZnO impurities, which is a well-established wide bandgap semiconductor.[11] Although the ultimate assignment of MOF-5 as a semiconductor or insulator is beyond the scope of this work, the results presented here emphasize the necessity of studying phase-pure materials as well as the utility of fluorescence spectroscopy for assessing the purity of MOFs.

We conclude that photoluminescence spectroscopy possesses distinct advantages for establishing MOF purity over typically employed powder XRD characterization methods, including simplicity, high speed, and a sensitivity to the presence of nanoscale semiconductor impurities, trapped charge-transfer species, and nonporous decomposition products. We expect that these results will have broad utility for evaluating the purity and possible semiconductor activity of other classes of MOFs, particularly those composed of tetrahedral Zn_4O_{13} building blocks.

Acknowledgment. This research was funded by the Defense Threat Reduction Agency under Contract 074325I-0 and by the U.S. Dept. of Energy Office of Proliferation Detection Programs. Sandia National Laboratories is a multiprogram laboratory managed and operated by Sandia Corporation, a wholly owned subsidiary of Lockheed Martin Corporation, for the National Nuclear Security Administration under Contract DE-AC04-94AL85000.

Supporting Information Available: Details of all experimental procedures, UV−vis absorption data, additional steady-state PL spectra, transmission electron micrographs, and details of the Scherrer equation. This material is available free of charge via the Internet at http://pubs.acs.org.

References

(1) Hafizovic, J.; Bjorgen, M.; Olsbye, U.; Dietzel, P. D. C.; Bordiga, S.; Prestipino, C.; Lamberti, C.; Lillerud, K. P. *J. Am. Chem. Soc.* **2007**, *129*, 3612.
(2) Chen, B.; Wang, X.; Zhang, Q.; Xi, X.; Cai, J. W.; Qi, H.; Shi, S. H.; Wang, J.; Yuan, D.; Fang, M. *J. Mater. Chem.* **2010**, *20*, 3758.
(3) Calleja, G.; Botas, J. A.; Orcajo, M. G.; Sanchez-Sanchez, M. *J. Porous Mater.* **2010**, *17*, 91.
(4) Huang, L.; Wang, H.; Chen, J.; Wang, Z.; Sun, J. C.; Zhao, D.; Yan, Y. *Microporous Mesoporous Mater.* **2003**, *58*, 105.
(5) Kaye, S. S.; Dailly, A.; Yaghi, O. M.; Long, J. R. *J. Am. Chem. Soc.* **2007**, *129*, 14176.
(6) Tranchemontagne, D. J.; Hunt, J. R.; Yaghi, O. M. *Tetrahedron* **2008**, *64*, 8553.
(7) Bordiga, S.; Lamberti, C.; Ricchiardi, G.; Regli, L.; Bonino, F.; Damin, A.; Lillerud, K. P.; Bjorgen, M.; Zecchina, A. *Chem. Commun.* **2004**, 2300.
(8) Alvaro, M.; Carbonell, E.; Ferrer, B.; Xamena, F.; Garcia, H. *Chem.—Eur. J.* **2007**, *13*, 5106.
(9) Tachikawa, T.; Choi, J. R.; Fujitsuka, M.; Majima, T. *J. Phys. Chem. C* **2008**, *112*, 14090.
(10) Silva, C. G.; Corma, A.; Garcia, H. *J. Mater. Chem.* **2010**, *20*, 3141.
(11) Xamena, F.; Corma, A.; Garcia, H. *J. Phys. Chem. C* **2007**, *111*, 80.
(12) Gascon, J.; Hernandez-Alonso, M. D.; Almeida, A. R.; van Klink, G. P. M.; Kapteijn, F.; Mul, G. *ChemSusChem* **2008**, *1*, 981.
(13) Mahata, P.; Madras, G.; Natarajan, S. *J. Phys. Chem. B* **2006**, *110*, 13759.
(14) Kobayashi, Y.; Jacobs, B.; Allendorf., M. D.; Long, J. R. *Chem. Mater.* **2010**, *22*, 4120.
(15) Civalleri, B.; Napoli, F.; Noel, Y.; Roetti, C.; Dovesi, R. *CrystEngComm* **2006**, *8*, 364.
(16) Bauer, C. A.; Timofeeva, T. V.; Settersten, T. B.; Patterson, B. D.; Liu, V. H.; Simmons, B. A.; Allendorf, M. D. *J. Am. Chem. Soc.* **2007**, *129*, 7136.
(17) Zhao, Z. X.; Li, Z.; Lin, Y. S. *Ind. Eng. Chem. Res.* **2009**, *48*, 10015.
(18) Hermes, S.; Schroder, F.; Amirjalayer, S.; Schmid, R.; Fischer, R. A. *J. Mater. Chem.* **2006**, *16*, 2464.
(19) Schrock, K.; Schroder, F.; Heyden, M.; Fischer, R. A.; Havenith, M. *Phys. Chem. Chem. Phys.* **2008**, *10*, 4732.
(20) Li, H.; Eddaoudi, M.; O'Keeffe, M.; Yaghi, O. M. *Nature* **1999**, *402*, 276.
(21) Rodriguez-Gattorno, G.; Santiago-Jacinto, P.; Rendon-Vazquez, L.; Nemeth, J.; Dekany, I.; Diaz, D. *J. Phys. Chem. B* **2003**, *107*, 12597.
(22) Uthirakumar, P.; Karunagaran, B.; Nagarajan, S.; Suh, E.-K.; Hong, C.-H. *J. Cryst. Growth* **2007**, *304*, 150.
(23) Kumbhakar, P.; Singh, D.; Tiwary, C. S.; Mitra, A. K. *Chalc. Lett.* **2008**, *5*, 387.
(24) Yang, S. J.; Park, C. R. *Nanotechnology* **2008**, *19*, 035609.
(25) Mo, C. M.; Li, Y. H.; Liu, Y. S.; Zhang, Y.; Zhang, L. D. *J. Appl. Phys.* **1998**, *83*, 4389.
(26) Pesika, N. S.; Stebe, K. J.; Searson, P. C. *J. Phys. Chem. B* **2003**, *107*, 10412.
(27) Muller, M.; Hermes, S.; Kaehler, K.; van den Berg, M. W. E.; Muhler, M.; Fischer, R. A. *Chem. Mater.* **2008**, *20*, 4576.
(28) Burrows, A. D.; Cassar, K.; Friend, R. M. W.; Mahon, M. F.; Rigby, S. P.; Warren, J. E. *CrystEngComm* **2005**, *7*, 548.
(29) Greathouse, J. A.; Allendorf, M. D. *J. Am. Chem. Soc.* **2006**, *128*, 10678.

JA1065625